ACS OMEGA

http://pubs.acs.org/journal/acsodf

Article

Electrochromic Displays via the Room-Temperature Electrochemical Oxidation of Nickel

Faiz Ali, Lakshman Neelakantan, and Parasuraman Swaminathan*

Cite This: *ACS Omega* 2022, 7, 39090−39096

Read Online

ACCESS | Metrics & More | Article Recommendations | Supporting Information

ABSTRACT: Electrochromism refers to the persistent and reversible change in color by applying an electric field. The phenomenon involves the insertion and extraction of electrons and ions within the active material. There is a keen interest in electrochromic (EC) materials, since they exhibit a wide range of potential applications. In recent years, transition-metal oxides have been widely investigated as EC materials due to their low power requirement, high coloration efficiency, and memory effect under an open-circuit condition. Nickel oxide (NiO), a p-type wide band gap semiconductor, exhibits attractive features such as a high color contrast ratio, good chemical stability, cost-effectiveness, and good compatibility with the cathodically coloring tungsten oxide. NiO thin films have been fabricated by various methods, but these are not cost-effective, scalable, or suitable for flexible applications. With the increasing demand for flexible and soft EC devices, it is essential to find routes to fabricate NiO thin films at lower temperatures. In this work, a NiO/Ni(OH)$_2$-based thin EC layer on fluorine-doped tin oxide-coated glass is developed via an electroless nickel (EN) deposition route, followed by room-temperature electrochemical oxidation. The deposition time is optimized to control the film thickness. The EC performance is investigated in an aqueous alkaline electrolyte (1 M KOH) by means of cyclic voltammetry, chronoamperometry, and transmittance measurements. Both the as-deposited and annealed films, after electrochemical oxidation, exhibit excellent EC properties with an optical modulation of approximately 64% (at 550 nm) and good response times of approximately 3 s (coloration) and 14 s (bleaching). A 2 × 2 display obtained by patterning the EN deposition is also demonstrated as part of this work.

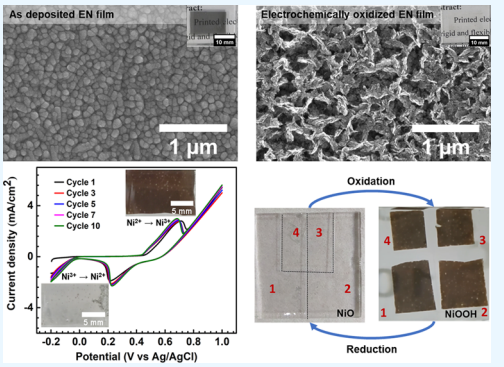

1. INTRODUCTION

Electrochromism is a phenomenon in which we can persistently and reversibly change the optical properties of a material by applying an electric field. The phenomenon involves the insertion and extraction of electrons or ions (H^+, Li^+, Na^+) within the electrochromic (EC) material.[1] EC materials can be used for applications including energy-saving smart windows, low-power informational displays, electronic papers, car self-dimming rear mirrors, e-skins, among several others.[2] Typical devices, such as smart windows, have a multilayered structure consisting of an EC film, an ion conductor, and an ion storage film sandwiched between two transparent conductors.[3] The EC layer is the core of the device and changes its color reversibly on the application of an electric field. Several organic and inorganic materials have been used as EC layers.[4−6] However, in recent years, transition-metal oxides (TMOs) have attracted a great deal of attention due to their low power requirement, high coloration efficiency (CE), and memory effect under open-circuit conditions.[4,7]

Principally, there are two different kinds of EC oxides; "cathodic coloring oxides" (W-, Ti-, Nb-, Mo-based) color upon charge insertion and "anodic coloring oxides" (Ni-, Cr-, Mn-, Fe-, Co-, Ir-, Rh-based) color upon de-insertion/extraction of charge.[6] Tungsten oxide (WO_3) is a widely studied cathodic coloring oxide due to its high optical modulation (OM) and CE and has been fabricated by a variety of techniques.[6] Among "anodically coloring" materials, nickel oxide (NiO) has been well studied. NiO thin films have been fabricated by a variety of physical (PVD) and chemical vapor deposition (CVD) techniques such as atomic layer deposition,[8] pulsed laser deposition,[9] sputter deposition,[10] thermal evaporation,[11] e-beam evaporation,[12] aerosol-assisted CVD,[13] and atmospheric pressure metal−organic CVD.[14] These deposition techniques are efficient in depositing thin films; however, they are vacuum intensive. Hence, the final products are costly, and large-scale manufacturing and deployment become challenging. Consequently, researchers have recently started exploring relatively economical solution-based techniques such as chemical bath deposition,[15] sol−gel deposition,[1] and spin coating[16] to synthesize high-quality NiO

Received: August 1, 2022
Accepted: October 10, 2022
Published: October 18, 2022

thin films. However, these processes often require high-temperature postannealing treatment of the films as an essential step. Thus, they cannot be extended to flexible polymer substrates such as poly(ethylene terephthalate) (PET) and polycarbonate (PC). However, with the increasing demand for flexible, stretchable, and soft devices for emerging EC applications such as foldable e-papers, smart clothes, and implantable displays,[17] it would be of interest to find suitable routes to fabricate high-quality NiO thin films at low temperatures.

Electroless nickel (EN) deposition is a chemical reduction technique commonly used to improve the corrosion resistance of metallic components.[18] It involves the chemical reduction of nickel (Ni), and the film thickness can be easily controlled by varying the deposition time.[19] In the present work, we have prepared a NiO-based thin film via room-temperature electrochemical oxidation of an EN thin film. Both the as-deposited and annealed films were used for electrochemical oxidation and morphological, optical, and EC studies were carried out to characterize the films. The results obtained for the films are better than previous reports on pure and doped nickel oxide films in terms of parameters such as OM, optical density change, and response time. The successful demonstration of the room-temperature synthesis of NiO-based EC films via electrochemical oxidation would pave the way for the fabrication of flexible electrochromic devices. A four-segment prototype EC display (2 × 2 structure) has also been successfully demonstrated in this work by creating a patterned EN film.

2. EXPERIMENTAL SECTION

2.1. Materials. All solvents and chemicals were of analytical grade and used without further purification. The fluorine-doped tin oxide (FTO)-coated glass (transmittance of 82.8% at 550 nm and sheet resistance of 15 Ω/sq.) was purchased from Techinstro, India. Nickel sulfate and potassium hydroxide pellets were obtained from Merck Life Sciences Pvt. Ltd., India. Sodium hypophosphite, sodium citrate, and ammonium sulfate were obtained from Avantor Performance Materials India Ltd. (India). All aqueous solutions were freshly prepared with deionized water.

2.2. Preparation of EC film. The FTO-coated glass was washed with acetone, ethanol, isopropyl alcohol (IPA), and finally deionized water in an ultrasonic bath for 7 min each at 50 °C. The substrate was masked with Kapton polyimide tape to create a window, of size 2 cm^2, for electroless deposition. This was followed by Au−Pd alloy sputter deposition using a Polaron Series SC7640 high-resolution sputter coater (Quorum Technologies) operating at 1 kV DC output and 25 mA process current for 60 s. This served as the activation layer for EN deposition.[19] The bath composition used was the same for all substrates[19,20] and is listed in Table S1. The bath temperature was fixed at 60 °C and controlled using an IKA C-MAG HS-7 digital hot plate and an attached thermocouple. The EN deposition was carried out for 30 s (referred to in this work as EN-30), followed by baking in an oven at 100 °C for 60 min to remove adsorbed moisture. This resulted in films with thickness of 21.6 nm. The films were then annealed in an ambient atmosphere at 350 °C for 60 min (the annealed sample is denoted as EN-30a). Then, the furnace was cooled to room temperature. Both the as-deposited and annealed EN films were electrochemically oxidized at room temperature to fabricate transparent films for the EC study.

A four-segment display (2 × 2 matrix) was also prepared as part of this work to demonstrate the patternability of this process. For this, the FTO film was divided into four sections using a diamond-coated scribe to create the matrix. Each section enclosed one segment and formed a path electrically isolated from the others. The sectioned FTO glass was then cleaned, masked using Kapton polyimide tape, and sputter coated with the Au−Pd alloy. After that, the EN deposition was carried out for 30 s. The postdeposition steps were the same as described above.

2.3. Characterization. The thickness of the thin films was recorded using a Bruker Contour GT Inmotion noncontact surface profiler. Morphological and qualitative chemical analyses were carried out using an Apreo S field-emission scanning electron microscope (FE-SEM) with the energy-dispersive spectroscopy (EDS) setup. The electrochemical experiments were performed in Biologic SP-150 and a Metrohm Autolab potentiostat. Electrochemical oxidation, cyclic voltammetry (CV), and chronoamperometry (CA) were carried out. A three-electrode system was used, with the EN film on FTO as the working electrode, Ag/AgCl (3 M KCl) as the reference electrode, and platinum grid as the counter electrode. The EN film was introduced into the cell and cycled between −0.2 and 1 V in 1 M KOH electrolyte at a scan rate of 20 mV/s up to 420 times to convert the Ni into Ni(II) oxide. Both the as-deposited and annealed EN films were subjected to this electrochemical oxidation. The kinetics of the coloration/bleaching switching behavior of the films was measured using CA by cycling between −0.2 and 1 V. The potential was applied for 30 s in each state for a total period of 390 s. The transmittance spectra of the films in the fully colored and fully bleached states were measured over the wavelength range from 300 to 800 nm with a Cary-5000 Agilent Ultraviolet−visible−near−infrared (UV−vis−NIR) spectrophotometer.

3. RESULTS AND DISCUSSION

3.1. Morphological Analysis. EN deposition proceeds in an island growth mode, with individual nuclei growing in size and coalescing to form a thin film.[20] A minimum deposition time is required to obtain a continuous stable film, and increasing the deposition time increases the film thickness. In this work, the deposition time was fixed at 30 s, since below that, discontinuous films were obtained and the color change during cycling exhibited a patchy behavior. Thicker films can be grown by increasing the deposition time. However, this causes a reduction in the transparency in the bleached state, and the film required more cycles for electrochemical oxidation. The obtained films have a granular morphology, as shown in Figures 1a and S1a. Also, the as-deposited films are amorphous in nature, which is normally attributed to the co-deposition of phosphorous.[19,20] To convert the amorphous film to crystalline, annealing is carried out, and previous studies indicate that films crystallize above 300 °C but tend to oxidize at temperatures above 400 °C.[21] Hence, an annealing temperature of 350 °C was used in this work to form crystalline nickel. The annealing does not seem to affect the film morphology, as seen in Figure 1a.

The EN films, as-deposited (EN-30) and annealed (EN-30a), were taken in an electrochemical cell and oxidized at room temperature by cycling between −0.2 and 1 V in a 1 M KOH electrolyte at 20 mV s^{-1} for 420 cycles. The potential range and the scan rate were adapted from the study by Firat et

https://doi.org/10.1021/acsomega.2c04859
ACS Omega 2022, 7, 39090−39096

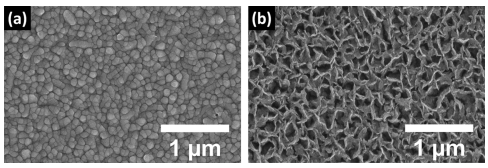

Figure 1. SEM images showing (a) granular morphology of the EN-30a film and (b) porous morphology of the same film after electrochemical oxidation. The granular morphology corresponds to the island growth mode, and this converts into the porous morphology due to repeated insertion/extraction of OH^- ions during oxidation.

al.[22] Before cycling, both the as-deposited and annealed films appeared gray, corresponding to primarily elemental nickel. During cycling, Ni electrooxidizes to Ni(II), resulting in the formation of NiO.[23] At the end of the process, the film appears completely transparent, suggesting that the oxidation is complete as seen in Figure S2. Figures 1b and S1b show representative SEM images of the EN film after electrochemical oxidation. A porous morphology can be seen, which can be attributed to the continuous insertion and extraction of OH^- ions in the film during cycling.[13,24] EDS data of the as-annealed and electrochemically oxidized film is presented in Table S2. Both Ni and P are present in the films, consistent with the electroless deposition process. The O, F, and Sn signals are from the substrate.

3.2. Electrochemical and Electrochromic Performance. *3.2.1. Cyclic Voltammetry Analysis.* Electrochemical oxidation of both the as-deposited and annealed films produced transparent films, as seen in Figure S2, corresponding to the formation of NiO.[23,25−27] These oxidized films were then used for the evaluation of the EC performance using CV measurements. Figure 2a,b compares the first 10 CV cycles of EN-30 and EN-30a thin films, respectively. The measurements were carried out in a 1 M KOH solution in the potential region of −0.2 to 1 V at a scan rate of 20 mV s^{-1}. The potential region is chosen based on the transparency of the obtained film. At −0.2 V the film appears fully transparent, while the colored state is complete at 1 V. Redox peaks corresponding to NiO could be seen in the voltammogram in both cases. In anodic polarization, NiO is reversibly oxidized into nickel oxyhydroxide (NiOOH), and the films switch from transparent to dark brown color. The peak indicates the oxidation of Ni^{2+} to Ni^{3+}, which is associated with OH^- insertion into the film. During cathodic polarization, the oxyhydroxide is reduced back to oxide, which corresponds to OH^- extraction, and the transparent state is obtained. The overall electrochemical reaction involved is provided in eqs 1[28] and 2[29,30]

$$Ni^{2+}O(\text{transparent}) + OH^- \underset{\text{reduction}}{\overset{\text{oxidation}}{\rightleftharpoons}} Ni^{3+}O(OH)(\text{colored}) + e^- \quad (1)$$

$$Ni^{2+}(OH)_2(\text{transparent}) + OH^- \underset{\text{reduction}}{\overset{\text{oxidation}}{\rightleftharpoons}} Ni^{3+}O(OH)(\text{colored}) + H_2O + e^- \quad (2)$$

This reversible switching between the transparent and colored states occurs in both the EN-30 and EN-30a samples. The main difference is that for the EN-30a film, there is a progressive increase in oxidation and reduction peak current intensity with the number of cycles, which indicates more charge penetration on the free sites of the active film surface.[22] However, for the EN-30 film, there is a progressive decrease in the oxidation and reduction peak current intensity, which indicates that this film has relatively lower cycling stability compared to the EN-30a film. The width of the anodic and cathodic peaks is found to be slightly narrower for EN-30 than that for EN-30a. This difference is found to be consistent across the different cycles. However, the coloration and bleaching times are diffusion-controlled processes and should depend more on the microstructure of the films, which are similar for EN-30 and EN-30a. These were evaluated by chronoamperometry analysis, as described in the next section.

3.2.2. Chronoamperometry Analysis. The optical modulation speed (namely, switching or response time) is an important indicator of the performance of an EC film. It is defined as the time required to reach 90% of the complete response. In this study, CA measurements were used to quantify the response time. Figure 3 shows the CA response of the EN-30 and EN-30a thin films under a potential of 1 V (coloration) and −0.2 V (bleaching). Each potential was applied for 30 s, for a total period of 390 s. The calculated response times for coloration (t_c) and bleaching (t_b) of the EN-30 film are 2.5 and 14.8 s, respectively, and those of the EN-30a film are 3.1 and 14.1 s, respectively. Interestingly, for the EN-30a film, while the coloration time was almost constant through the subsequent application of the square-waved potential, the bleaching time was seen to reduce, going from 14.1 s during the 60−90 s interval to 6.7 s during the 360−390 s interval (Table S3). The response data are compared in

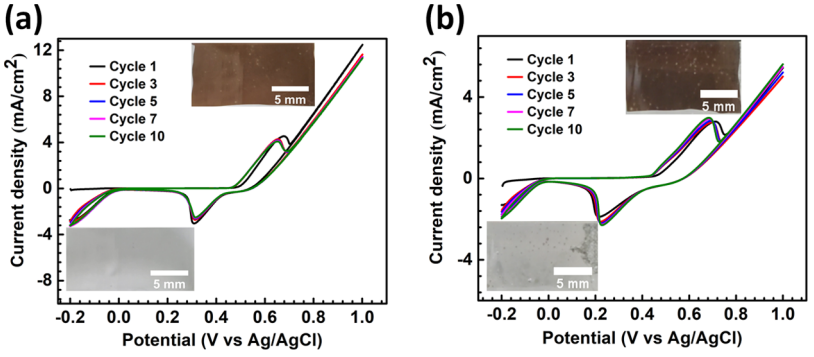

Figure 2. Cyclic voltammetry profiles for (a) EN-30 and (b) EN-30a film, obtained in 1 M aqueous KOH at a scan rate of 20 mV s^{-1} and in the range of −0.2−1 V at room temperature. A stable profile can be seen for the annealed sample, while the peak intensity reduces for the as-deposited sample with the increasing number of cycles.

https://doi.org/10.1021/acsomega.2c04859
ACS Omega 2022, 7, 39090−39096

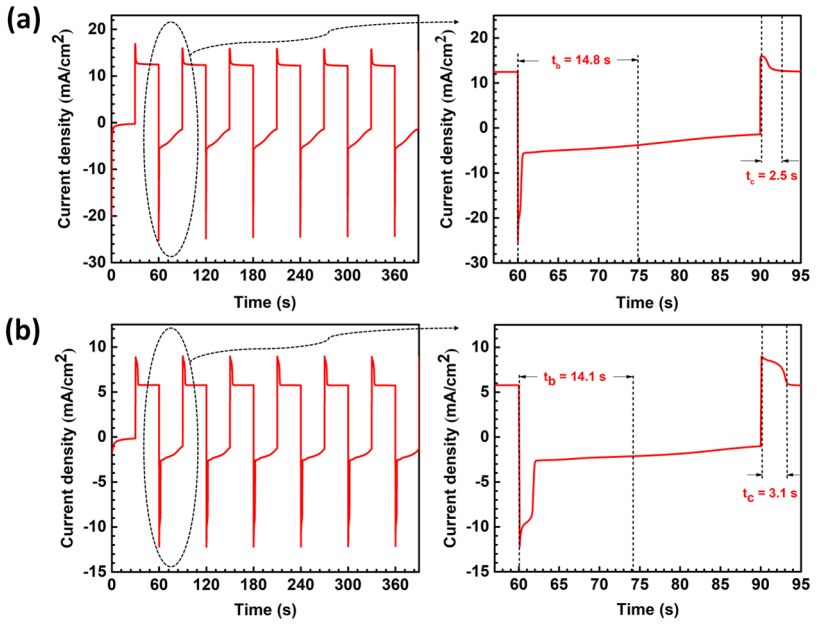

Figure 3. Chronoamperometric curves of (a) EN-30 and (b) EN-30a films. A potential of 1 V is used for coloring and −0.2 V for bleaching with a time step of 30 s. The electrolyte used is 1 M KOH. One curve is expanded for each film (on the right), showing the calculation of coloration and bleaching times for the films. The large bleaching times are attributed to the large tail in the plots.

Table 1. Comparison of the Optical Performance of NiO EC Films from Literature with Data from This Work

film	deposition method	OM (%)	response time t_c (s)	response time t_b (s)	ΔOD	CE (cm^2/C)
N-doped Ni oxide[36]	radio frequency magnetron sputtering		18.7	14.5		33.0
Cu-doped Ni oxide[22]	electrodeposition	57.1	2.3	1.8		13.8
Ni hydroxide[37]	galvanostatic electrochemical reduction	83.2	12	9.5	0.8	29.0
Ni oxide[38]	electrodeposition		1.7	2.0	0.7	107
nanoparticulate Ni oxide[39]	dip coating	38.9		1.2	0.3	
Ni oxide[40]	E-beam evaporation	38.8				24.8
Zn-doped Ni oxide[41]	sol−gel spin coating	59.8	3.0	8.0	0.5	33.6
Ni oxide nanorod array[42]	hot-filament metal-oxide vapor deposition technique	60.0	1.6	1.2	1.1	43.3
electrochemically oxidized EN (EN-30)—this work	electroless nickel deposition	64.4	2.5	14.8	0.7	6.3
electrochemically oxidized annealed EN (EN-30a)—this work	electroless nickel deposition	64.3	3.1	14.1	0.9	12.0

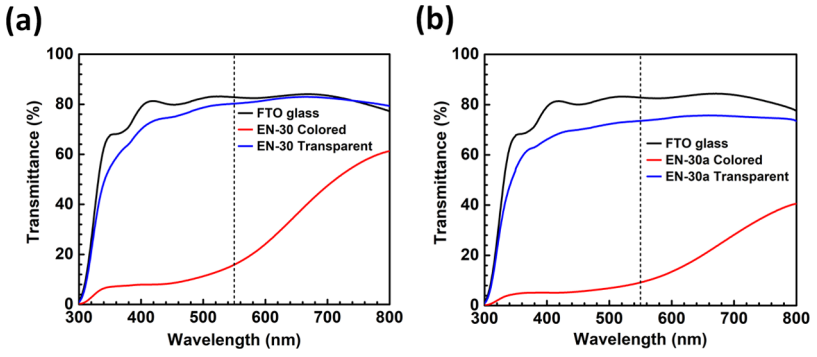

Figure 4. UV−vis transmittance spectra of (a) EN-30 thin film and (b) EN-30a thin film, showing colored (1 V) and transparent (−0.2 V) states. The dotted line represents the wavelength at which the OM is calculated, i.e., 550 nm. The transmittance of the bare FTO glass is also included for comparison.

Table 1 with NiO films produced by other routes and the coloration times are better than those observed previously. The relatively faster reaction kinetics can be attributed to the highly porous morphology of the oxidized films (Figures 1b and S2b). This facilitates electrolyte penetration, providing a large electrode/electrolyte contact area and a short diffusion length for the ions.[28,31] Previous electrochemical impedance spectroscopy (EIS) studies on NiO films also support the

https://doi.org/10.1021/acsomega.2c04859
ACS Omega 2022, 7, 39090−39096

conclusion that the porous structure has lower charge transfer and ion diffusion resistance.[32,33]

3.2.3. Optical Properties. OM, change in optical density, and CE are other important parameters for comparing EC films. OM describes the difference in the transmittance of the film in the transparent and colored states and is expressed by eq 3

$$\mathrm{OM} = (T_b - T_c)_\lambda \tag{3}$$

where T_b and T_c are the transmittances for the bleached and colored states, respectively, and λ is the wavelength at which the modulation is measured, usually 550 nm. The change in optical density (ΔOD) is calculated as per eq 4

$$\Delta\mathrm{OD} = \log(T_b/T_c)_\lambda \tag{4}$$

CE is defined as the ratio of ΔOD at a specific wavelength and the charge inserted (or extracted) per unit electrode area (Q). A film with high CE is preferred since only a small amount of charge is then required to cause optical modulation. CE is calculated as per eq 5[22,34,35]

$$\mathrm{CE} = (\Delta\mathrm{OD})_\lambda/Q = \log(T_b/T_c)_\lambda/Q \tag{5}$$

and Q is calculated as per eq 6

$$Q = \int_{t_1}^{t_2} j\,\mathrm{d}t \tag{6}$$

where j is the current density and t_1 and t_2 are the starting and ending times of the coloration or bleaching process.

Figure 4 shows the transmittance curves of both EN-30 and EN-30a thin films. The coloring voltage used is 1 V, and the bleaching voltage is −0.2 V. Using eq 3, OM of the EN-30 thin film, at a wavelength of 550 nm, was calculated to be 64.4% (with a transmittance of 80.3% in its bleached state and 15.9% in its colored state), and that for the EN-30a film was calculated to be 64.3% (with a transmittance of 73.5% in its bleached state and 9.2% in its colored state). The OM values for both EN-30 and EN-30a are similar, reflecting the similar morphologies of the oxidized films. It should be noted that the transmittance data mentioned here includes the transmittance through the substrate (FTO-coated glass), which has a value of 82.8% at 550 nm and is included in Figure 4. OD change is calculated using eq 4 and found to be 0.7 for the EN-30 film and 0.9 for the EN-30a film.

Both cathodic and anodic charge densities (Q_c and Q_a) were calculated by integrating the area under the current density vs the time curve obtained from the CA experiment (Figure 3). CE for the EN-30 film was calculated to be 6.3 cm^2/C using cathodic charge density (Q_c = 111.0 mC/cm^2) and change in optical density at 550 nm ($(\Delta OD)_{\lambda = 550\ nm}$ = 0.7) and that for the EN-30a film was calculated to be 12.0 cm^2/C using cathodic charge density (Q_c = 75.4 mC/cm^2) and change in optical density at 550 nm ($(\Delta OD)_{\lambda = 550\ nm}$ = 0.9).

Table 1 compares the electrochromic performance of EN thin films deposited as a part of this work with NiO-based thin films deposited using different routes. The difference in properties can be attributed to the morphology of the films that are produced. EN deposition produces films with a granular morphology, arising from the island growth mode of the EN film. During electrochemical oxidation, the insertion and de-insertion of OH^- ions transform the film into a porous morphology. This porous morphology helps in fast coloration and bleaching. Compared to the porous morphology produced in electrochemical oxidation, the films produced by physical routes such as sputtering tend to have columnar grains, which leads to a large coloration time.

In Table 1, the electrochromic comparison is made using the parameters OM, response time, ΔOD, and CE. As can be seen in the table, the OM of the EN thin films developed in this work is higher compared to that of NiO films prepared by other routes. The OD values are also comparable to other films. While the coloration times are short, the bleaching time seems long and only found to be better than the films prepared by sputtering. One reason for this long bleaching time is due to the tail (see Figure 3) in the CA curves and the fact that the time is defined based on reaching 90% of the response. If we calculate the time required to reach 85% of the complete response, then it works out to be 5.0 s (t_b) for EN-30 and 2.0 s (t_b) for EN-30a. Similarly, if we calculate the time required to reach 80% of the complete response, then it works out to be 0.6 s (t_b) for EN-30 and 1.8 s (t_b) for EN-30a. This clearly shows that both EN-30 and EN-30a films have rapid switching kinetics.

The study shows that annealing the as-deposited film before electrochemical oxidation improves the stability of the films but provides no significant improvement in other EC properties such as OM and response time. This result paves the way for developing EC films on flexible substrates such as poly(ethylene terephthalate) (PET), which cannot withstand temperatures higher than 150 °C. By patterning the EN deposition process, it is possible to form passive matrix-type monochrome display devices.

3.3. Four-Segment Electrochromic-Based Display. EN deposition requires an activation layer on nonferrous substrates prior to deposition. Typically, Pd is used as the activation layer by coating from a solution containing a mixture of palladium and tin chloride.[43,44] Recently, we showed that EN deposition can be activated using a sputtered Au−Pd activation layer. This allows for combining EN deposition with the conventional photolithography process to form patterned films.[19] This concept can be extended to form pixel-based EC films by combining patterned EN deposition, followed by electrochemical oxidation. As a proof of concept, a four-segment (2 × 2) EN layer was created, as described in Section 2.3. Masking was used to define four segments on the FTO substrate, where Au−Pd was sputtered. Deposition occurred only in the sputtered areas, and the NiO was obtained after annealing and electrochemical oxidation, as seen in Figure 5a.

Electrical connections were made such that each element of the display can be controlled individually or in combination with others for the coloring and bleaching process. Both individual and combined activation of the display elements are demonstrated in Figure 5b,c, respectively. A video of the process is available in Supporting Information, Video S1. This demonstration shows that the EN deposition method combined with Au−Pd sputter coating could be successfully employed to make multipixel displays that could be switched on or off individually to produce different images.

4. CONCLUSIONS

Nickel oxide based thin films have been successfully prepared on FTO-coated glasses by the electrochemical oxidation of EN films. Both as-deposited and annealed EN thin films were converted into oxide by electrochemical oxidation, and the films exhibited a highly porous morphology. Both the as-deposited and annealed films exhibited a uniform and high

https://doi.org/10.1021/acsomega.2c04859
ACS Omega 2022, 7, 39090−39096

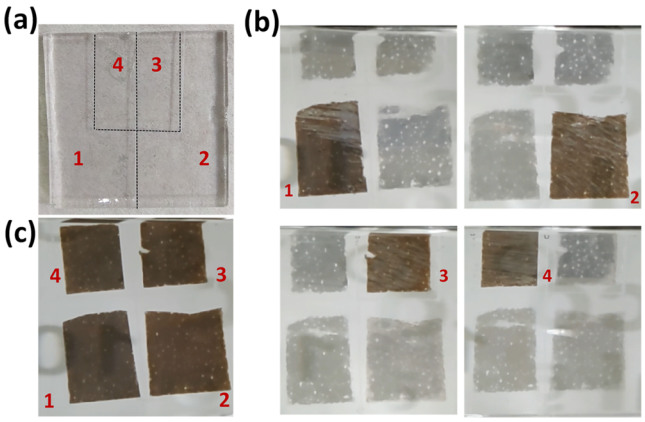

Figure 5. (a) Electrochemically oxidized four-segment EC display. (b) Each electrochromic segment is controlled individually without influencing the remaining segments. (c) All four segments are controlled at the same time.

optical modulation of around 64%. They also exhibited fast switching kinetics with coloration and bleaching times of 2.5 and 14.8 s for the as-deposited film, respectively, and 3.1 and 14.1 s for the annealed film, respectively. The annealed films exhibited slightly better OD and CE when compared with the as-deposited film. The excellent EC properties of the electrochemically oxidized EN films can be attributed to the highly porous structure. This facilitates electrolyte penetration, providing a large electrode/electrolyte contact area and a shorter diffusion length of ions, leading to lower inner resistance and faster reaction kinetics. A four-segment EC display was prepared to exhibit the potential of this approach. In conclusion, this work provides an easy and effective method for synthesizing nickel oxide based thin films with high EC performance, suitable for fabricating flexible electrochromic windows and displays. Future work will focus on developing EC displays using solid-state polymer electrolytes and suitable transparent counter electrodes.

■ ASSOCIATED CONTENT

Supporting Information

The Supporting Information is available free of charge at https://pubs.acs.org/doi/10.1021/acsomega.2c04859.

Working of the four-segment electrochromic display; composition of electroless nickel bath; EDS data on the thin films; coloration and bleaching times of the EN-30a film in different time ranges; morphology of EN-30 films before and after electrochemical oxidation, and images of electroless nickel thin films on FTO-coated glass substrates before and after electrochemical oxidation (PDF)

Working of 4-segment electrochromic display (Video S1) (AVI)

■ AUTHOR INFORMATION

Corresponding Author

Parasuraman Swaminathan − *Department of Metallurgical and Materials Engineering, Electronic Materials and Thin Films Lab, IIT Madras, Chennai 600036, India; Ceramics Technologies Group-Center of Excellence in Materials and Manufacturing for Futuristic Mobility, IIT Madras, Chennai 600036, India;* orcid.org/0000-0002-9821-3981; Email: swamnthn@iitm.ac.in

Authors

Faiz Ali − *Department of Metallurgical and Materials Engineering, Electronic Materials and Thin Films Lab, IIT Madras, Chennai 600036, India; Department of Metallurgical and Materials Engineering, Corrosion Engineering and Materials Electrochemistry Lab, IIT Madras, Chennai 600036, India*

Lakshman Neelakantan − *Department of Metallurgical and Materials Engineering, Corrosion Engineering and Materials Electrochemistry Lab and Ceramics Technologies Group-Center of Excellence in Materials and Manufacturing for Futuristic Mobility, IIT Madras, Chennai 600036, India*

Complete contact information is available at: https://pubs.acs.org/10.1021/acsomega.2c04859

Author Contributions

F.A. designed the experiments, synthesized and characterized the films, and prepared the first draft of the manuscript. L.N. and P.S. supervised and coordinated this study and revised the manuscript.

Notes

The authors declare no competing financial interest.

■ ACKNOWLEDGMENTS

The work was supported by IIT Madras under the Institute of Eminence Research Initiative Project on Materials and Manufacturing for Futuristic Mobility (project no. SB20210850MMMHRD008275).

■ REFERENCES

(1) Dalavi, D. S.; Devan, R. S.; Patil, R. S.; Ma, Y.; Patil, P. S. Electrochromic Performance of Sol-Gel Deposited NiO Thin Film. *Mater. Lett.* **2013**, *90*, 60−63.

(2) Granqvist, C. G. Electrochromics for Smart Windows: Oxide-Based Thin Films and Devices. *Thin Solid Films* **2014**, *564*, 1−38.

(3) Cai, G.; Wang, J.; Lee, P. S. Next-Generation Multifunctional Electrochromic Devices. *Acc. Chem. Res.* **2016**, *49*, 1469−1476.

(4) Zhang, W.; Li, H.; Hopmann, E.; Elezzabi, A. Y. Nanostructured Inorganic Electrochromic Materials for Light Applications. *Nanophotonics* **2020**, *10*, 825−850.

(5) Li, J.; Zhuang, Y.; Chen, J.; Li, B.; Wang, L.; Liu, S.; Zhao, Q. Two-Dimensional Materials for Electrochromic Applications. *EnergyChem* **2021**, *3*, No. 100060.

(6) Niklasson, G. A.; Granqvist, C. G. Electrochromics for Smart Windows: Thin Films of Tungsten Oxide and Nickel Oxide, and Devices Based on These. *J. Mater. Chem.* **2007**, *17*, 127−156.

(7) Wu, W.; Wang, M.; Ma, J.; Cao, Y.; Deng, Y. Electrochromic Metal Oxides: Recent Progress and Prospect. *Adv. Electron. Mater.* **2018**, *4*, No. 1800185.

(8) Thimsen, E.; Martinson, A. B. F.; Elam, J. W.; Pellin, M. J. Energy Levels, Electronic Properties, and Rectification in Ultrathin p-NiO Films Synthesized by Atomic Layer Deposition. *J. Phys. Chem. C* **2012**, *116*, 16830−16840.

(9) Yang, M.; Pu, H.; Zhou, Q.; Zhang, Q. Transparent P-Type Conducting K-Doped NiO Films Deposited by Pulsed Plasma Deposition. *Thin Solid Films* **2012**, *520*, 5884−5888.

(10) Chen, S. C.; Wen, C. K.; Kuo, T. Y.; Peng, W. C.; Lin, H. C. Characterization and Properties of NiO Films Produced by Rf Magnetron Sputtering with Oxygen Ion Source Assistance. *Thin Solid Films* **2014**, *572*, 51−55.

(11) Kaya, D.; Aydınoğlu, H. S.; Tüzemen, E. S.; Ekicibil, A. Investigation of Optical, Electronic, and Magnetic Properties of p-Type NiO Thin Film on Different Substrates. *Thin Solid Films* **2021**, *732*, No. 138800.

(12) Kuanr, S. K.; Vinothkumar, G.; Babu, K. S. Substrate Temperature Dependent Structural Orientation of EBPVD Deposited NiO Films and Its Influence on Optical, Electrical Property. *Mater. Sci. Semicond. Process.* **2018**, *75*, 26−30.
(13) Sialvi, M. Z.; Mortimer, R. J.; Wilcox, G. D.; Teridi, A. M.; Varley, T. S.; Wijayantha, K. G. U.; Kirk, C. A. Electrochromic and Colorimetric Properties of Nickel(II) Oxide Thin Films Prepared by Aerosol-Assisted Chemical Vapor Deposition. *ACS Appl. Mater. Interfaces* **2013**, *5*, 5675−5682.
(14) Roffi, T. M.; Nozaki, S.; Uchida, K. Growth Mechanism of Single-Crystalline NiO Thin Films Grown by Metal Organic Chemical Vapor Deposition. *J. Cryst. Growth* **2016**, *451*, 57−64.
(15) Xia, X. H.; Tu, J. P.; Zhang, J.; Wang, X. L.; Zhang, W. K.; Huang, H. Electrochromic Properties of Porous NiO Thin Films Prepared by a Chemical Bath Deposition. *Sol. Energy Mater. Sol. Cells* **2008**, *92*, 628−633.
(16) Zrikem, K.; Song, G.; Aghzzaf, A. A.; Amjoud, M.; Mezzane, D.; Rougier, A. UV Treatment for Enhanced Electrochromic Properties of Spin Coated NiO Thin Films. *Superlattices Microstruct.* **2019**, *127*, 35−42.
(17) Yan, C.; Kang, W.; Wang, J.; Cui, M.; Wang, X.; Foo, C. Y.; Chee, K. J.; Lee, P. S. Stretchable and Wearable Electrochromic Devices. *ACS Nano* **2014**, *8*, 316−322.
(18) Brenner, A.; Riddell, G. E. Nickel Plating on Steel by Chemical Reduction. *J. Res. Natl. Bur. Stand.* **1946**, *37*, 31−34.
(19) Chakraborty, A.; Nair, N. M.; Adekar, A.; Swaminathan, P. Templated Electroless Nickel Deposition for Patterning Applications. *Surf. Coat. Technol.* **2019**, *370*, 106−112.
(20) Narayanan, M.; Harsha, A.; Chakraborty, A.; Swaminathan, P. Reactive Bilayers by Self-Activated Electroless Nickel-Phosphorous Deposition on Pure Aluminum. *JOM* **2021**, *73*, 574−579.
(21) Sribalaji, M.; Arunkumar, P.; Babu, K. S.; Keshri, A. K. Crystallization Mechanism and Corrosion Property of Electroless Nickel Phosphorus Coating during Intermediate Temperature Oxidation. *Appl. Surf. Sci.* **2015**, *355*, 112−120.
(22) Firat, Y. E.; Peksoz, A. Efficiency Enhancement of Electrochromic Performance in NiO Thin Film via Cu Doping for Energy-Saving Potential. *Electrochim. Acta* **2019**, *295*, 645−654.
(23) Lampert, C. M.; Omstead, T. R.; Yu, P. C. Chemical and Optical Properties of Electrochromic Nickel Oxide Films. *Sol. Energy Mater.* **1986**, *14*, 161−174.
(24) Wang, W.; Li, Z.; Yu, Z.; Su, G. The Stabilization of Ni(OH)2 by In2O3 Rods and the Electrochromic Performance of Ni(OH)2/In2O3-Rod Composite Porous Film. *Thin Solid Films* **2021**, *734*, No. 138839.
(25) Alsabet, M.; Grdeń, M.; Jerkiewicz, G. Electrochemical Growth of Surface Oxides on Nickel. Part 2: Formation of β-Ni(OH)2 and NiO in Relation to the Polarization Potential, Polarization Time, and Temperature. *Electrocatalysis* **2014**, *5*, 136−147.
(26) Alsabet, M.; Grdeń, M.; Jerkiewicz, G. Electrochemical Growth of Surface Oxides on Nickel. Part 3: Formation of β-NiOOH in Relation to the Polarization Potential, Polarization Time, and Temperature. *Electrocatalysis* **2015**, *6*, 60−71.
(27) Seghiouer, A.; Chevalet, J.; Barhoun, A.; Lantelme, F. Electrochemical Oxidation of Nickel in Alkaline Solutions: A Voltammetric Study and Modelling. *J. Electroanal. Chem.* **1998**, *442*, 113−123.
(28) Yuan, Y. F.; Xia, X. H.; Wu, J. B.; Chen, Y. B.; Yang, J. L.; Guo, S. Y. Enhanced Electrochromic Properties of Ordered Porous Nickel Oxide Thin Film Prepared by Self-Assembled Colloidal Crystal Template-Assisted Electrodeposition. *Electrochim. Acta* **2011**, *56*, 1208−1212.
(29) Zhu, L.; Ong, W. L.; Lu, X.; Zeng, K.; Fan, H. J.; Ho, G. W. Substrate-Friendly Growth of Large-Sized $Ni(OH)_2$ Nanosheets for Flexible Electrochromic Films. *Small* **2017**, *13*, No. 1700084.
(30) Kadam, L. D.; Patil, P. S. Studies on Electrochromic Properties of Nickel Oxide Thin films Prepared by Spray Pyrolysis Technique. *Sol. Energy Mater. Sol. Cells* **2001**, *69*, 361−369.
(31) Cai, G.; Cui, M.; Kumar, V.; Darmawan, P.; Wang, J.; Wang, X.; Lee-Sie Eh, A.; Qian, K.; Lee, P. S. Ultra-Large Optical Modulation of Electrochromic Porous WO3 Film and the Local Monitoring of Redox Activity. *Chem. Sci.* **2016**, *7*, 1373−1382.
(32) Xia, X. H.; Tu, J. P.; Zhang, J.; Wang, X. L.; Zhang, W. K.; Huang, H. Morphology effect on the electrochromic and electrochemical performances of NiO thin films. *Electrochim. Acta* **2008**, *53*, 5721−5724.
(33) Huang, H.; Tian, J.; Zhang, W. K.; Gan, Y. P.; Tao, X. Y.; Xia, X. H.; Tu, J. P. Electrochromic properties of porous NiO thin film as a counter electrode for NiO/WO_3 complementary electrochromic window. *Electrochim. Acta* **2011**, *56*, 4281−4286.
(34) Korošec, R. C.; Bukovec, P.Sol-Gel Prepared NiO Thin Films for Electrochromic Applications*Acta Chim. Slov*200653136147http://acta-arhiv.chem-soc.si/53/53-2-136(int).pdf
(35) Shi, J.; Lai, L.; Zhang, P.; Li, H.; Qin, Y.; Gao, Y.; Luo, L.; Lu, J. Aluminum Doped Nickel Oxide Thin Film with Improved Electrochromic Performance from Layered Double Hydroxides Precursor in Situ Pyrolytic Route. *J. Solid State Chem.* **2016**, *241*, 1−8.
(36) Lin, F.; Gillaspie, D. T.; Dillon, A. C.; Richards, R. M.; Engtrakul, C. Nitrogen-Doped Nickel Oxide Thin Films for Enhanced Electrochromic Applications. *Thin Solid Films* **2013**, *527*, 26−30.
(37) Mortimer, R. J.; Sialvi, M. Z.; Varley, T. S.; Wilcox, G. D. An in Situ Colorimetric Measurement Study of Electrochromism in the Thin-Film Nickel Hydroxide/Oxyhydroxide System. *J. Solid State Electrochem.* **2014**, *18*, 3359−3367.
(38) Sonavane, A. C.; Inamdar, A. I.; Shinde, P. S.; Deshmukh, H. P.; Patil, R. S.; Patil, P. S. Efficient Electrochromic Nickel Oxide Thin Films by Electrodeposition. *J. Alloys Compd.* **2010**, *489*, 667−673.
(39) Sun, D. L.; Zhao, B. W.; Liu, J. B.; Wang, H.; Yan, H. Application of Nickel Oxide Nanoparticles in Electrochromic Materials. *Ionics* **2017**, *23*, 1509−1515.
(40) Guo, X.; Wang, W.; Wen, R. T. Enhanced Electrochromic Performance by Anodic Polarization in Nickel Oxide Films. *Crystals* **2021**, *11*, No. 615.
(41) Kim, K. H.; Kahuku, M.; Abe, Y.; Kawamura, M.; Kiba, T. Improved Electrochromic Performance in Nickel Oxide Thin Film by Zn Doping. *Int. J. Electrochem. Sci.* **2020**, *15*, 4065−4071.
(42) Patil, R. A.; Devan, R. S.; Lin, J. H.; Ma, Y. R.; Patil, P. S.; Liou, Y. Efficient Electrochromic Properties of High-Density and Large-Area Arrays of One-Dimensional NiO Nanorods. *Sol. Energy Mater. Sol. Cells* **2013**, *112*, 91−96.
(43) Sudagar, J.; Lian, J.; Sha, W. Electroless Nickel, Alloy, Composite and Nano Coatings - A Critical Review. *J. Alloys Compd.* **2013**, *571*, 183−204.
(44) Khoperia, T. N. Investigation of the Substrate Activation Mechanism and Electroless Ni-P Coating Ductility and Adhesion. *Microelectron. Eng.* **2003**, *69*, 391−398.

https://doi.org/10.1021/acsomega.2c04859
ACS Omega 2022, 7, 39090−39096